

Article

# Zircon as a Mineral Indicating the Stage of Granitoid Magmatism at Northern Chukotka, Russia

Viktor I. Alekseev \*  and Ivan V. Alekseev

Faculty of Geological Prospecting, Saint-Petersburg Mining University, 2, 21st Line, 199106 St Petersburg, Russia; alekseev\_iv@pers.spmi.ru

\* Correspondence: alekseev\_vi@pers.spmi.ru

Received: 9 April 2020; Accepted: 18 May 2020; Published: 20 May 2020



**Abstract:** A comparative study of the zircon composition and texture in granites of a three-stage Late Cretaceous magmatism in the Chaun area, Chukotka, Russia, was conducted in biotite granites (BG), quartz monzonites-monzogranites (MG), and zinnwaldite granites (ZG). The significance of the study entails determining the mineralogical indicators of similar granitoids in areas of multi-stage petrogenesis. It is shown that in the rock series of Northern Chukotka, BG → MG → ZG, a morphological evolution of zircon takes place: a reduction in size, elongation, a growing complexity of the crystallography, and an individual texture. In later generations of zircon, as a result of the recrystallization and metasomatism, rare-metal overgrowths, defects in the crystal structure, pores and fissures, and mineral inclusions appear, whereas the crystal-face indices and patterns become more complicated. We can observe the geochemical evolution of zircon: a gradual change in the concentration of trace elements (Hf, U, Y, Th, Nb, and Ti), rare earth elements (Yb, Er, and Dy, as well as Ce and Nd), and uncommon elements (Ca and Al). Rare elements (REE, Y, Hf, Nb, U, and Th) at the post-magmatic stage of the regional history acquired economic abundances. Zircon is therefore indicative of productive ore-magmatic systems.

**Keywords:** zircon; biotite granite; monzogranite; zinnwaldite granite; ongonite; North Chukotka; Russia

## 1. Introduction

Many researchers have noted the evolution of rock-forming minerals in the granitoids of the Chukchi Peninsula. However, the evolution of accessory minerals has not been studied. A number of common accessory minerals, such as zircon, is recognized to be indicators of granitoids petrogenesis conditions, as well as of their age [1–3].

The determination of the mineralogical indicators of granitoids is relevant in the regions of post-orogenic magmatism, where repeated formation of granitoids of similar age and composition, combined in large plutons, occurred. These regions include Northern Chukotka, which is characterized by the facies diversity of its synchronous granitoids and the similarity of its heterochronous rocks composition [4,5]. The paper conveys a comparative analysis of zircons from granitoids of three Late Cretaceous magmatic stages in the Chaun area, Chukotka, namely biotitic granites, monzogranites, and zinnwaldite granites.

## 2. Geological Setting

The Chaun area is located on the eastern coast of the Chaun bay, and includes granitoids of the Chukotka plutonic belt. Containing rocks are mainly represented by clay slates, siltstones, and sandstones of the Upper Triassic and Jurassic systems. They form the Palyava synclinorium with a north-west strike. Mesozoic folded structures are molded in conditions of passive continental margins [6]. Granitoids occupy over 900 km<sup>2</sup>, which is more than 20% of the territory surface. The largest

intrusions of the area occupy from 30 to 270 km<sup>2</sup>: Shelag, Kuiviveem, Yanranay, Inroginay, Pevek, Lootaypin, Pyrkanayan, Severnyi, Pytlyan, and Palyan. The late orogenic gabbro-diorit-granodiorite, granodiorite-granite, and granite-leucogranite intrusions of the Late Jurassic-Early Cretaceous form the granodiorite-granite complex of Chukotka. The greatest plutons are mostly comprised of post-orogenic complexes: Chaun granite, Ichuveem quartz monzonite-monzogranite and Pyrkakay complex of rare metal zinnwaldite granites and ongonites, namely topaz-bearing albite-rich microgranites [4,5]. Ten large deposits, and more than 100 ore occurrences and placers of tin, gold, and rare-metals, are attributed to the Late Cretaceous granitoids: Valkumey, Prospector, Kekura, Palyan, Pyrkakay, Iultin, etc. (Figure 1).

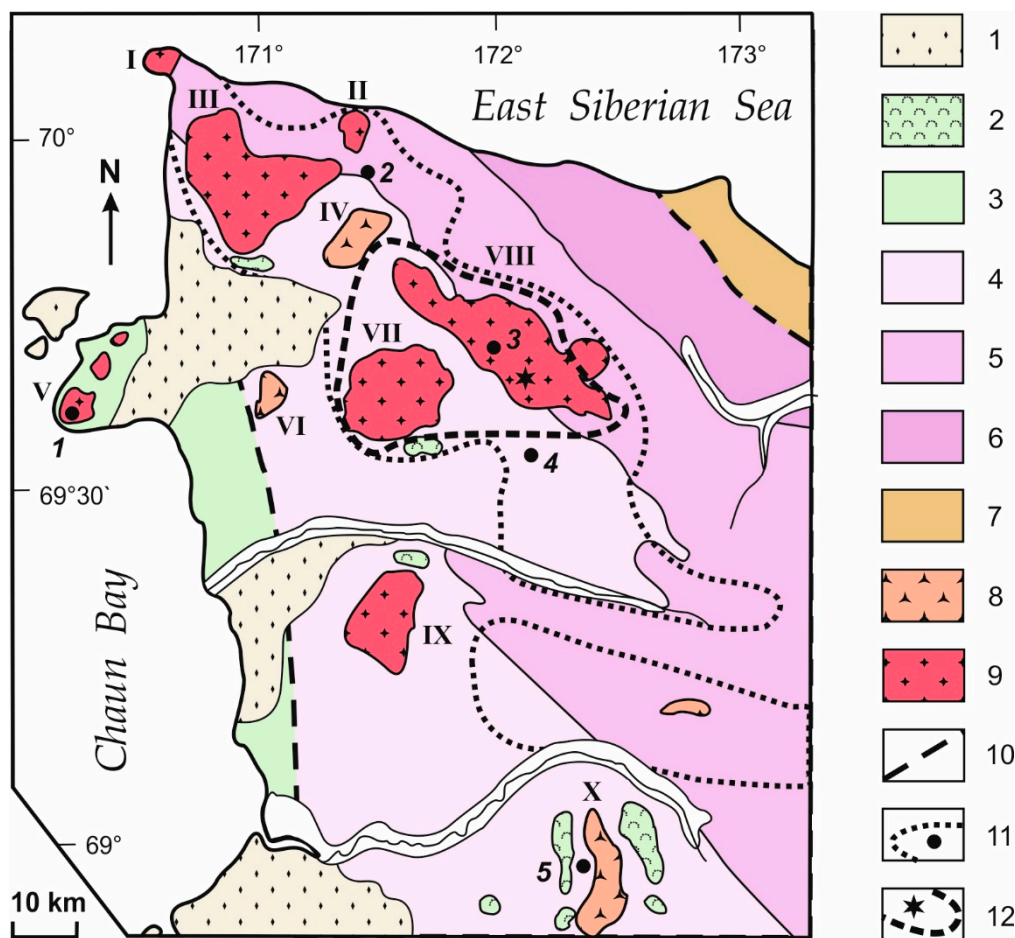


**Figure 1.** The geological map of the Chaun district, Northern Chukotka: 1—Upper Quaternary deposits; 2—Upper Cretaceous volcanics: basalts, andesites, rhyolites; 3–6—Mesozoic terrigenous-clay deposits of the Palyavaam synclinorium: 3—Valanginian stage, 4—Norian stage, 5—Carnian stage, 6—deposits of the Lower and the Middle Triassic; 7—Paleozoic sandstones and limestones of the Pegtymel anticlinorium; 8—intrusions of MG (Ichuveem complex); 9—intrusions of BG (Chaun complex); 10—disjunctive dislocations; 11—borders of the Chaun cryptotatolite; circles and Arabic numerals—deposits: 1—Valcumei, 2—Prospector, 3—Kekura, 4—Pyrkakay, and 5—Palyan; 12—area of small intrusions of ZG (star—position of the Kuluveem stock of ZG, Pyrkakay complex). Roman numerals—intrusions: I—Shelag, II—Kuiviveem, III—Yanranay, IV—Inroginay, V—Pevek, VI—Lootaypin, VII—Pyrkanayan, VIII—Severnyi, IX—Pytlyan, and X—Palyan.

Zircon for this study was sampled from the North Chukotka granitoids that comprise the three Late Cretaceous stages: biotitic granites (Chaun complex), quartz monzonites and monzogranites (Ichuveem complex), as well as zinnwaldite granites (Pyrkakay complex). According to SHRIMP-II mass spectrometry, the U-Pb ages of zircon from the complexes are 1)  $89.4 \pm 0.7$  Ma, 2)  $84.3 \pm 0.7$  Ma,

and 3)  $84.1 \pm 0.6$  Ma, respectively [5]. According to geological data, zinnwaldite granites are intruded after quartz monzonites and monzogranites.

Biotite granites (BG) of the calc-alkaline series are widely known within polyformational plutons, such as intrusions in Pevek, Pyrkanayan, Severnyi, and Iultin. Spatially they are combined with Early Cretaceous granodiorites and adamellites, which are often referred to the early phase of the granite complex. BG appear as medium-sized hypabyssal intrusions (100–300 km<sup>2</sup>), discordant to folding and elongated along magma-controlling faults. According to geophysical data, the accumulation of granitoid plutons marks the position of the deeply hidden Chaun granite cryptobatholith. There are also small (< 100 km<sup>2</sup>) stock- and laccolith-like intrusive bodies—Solnechny, Svetly, Kuiviveem, etc. BG massifs have a three-facies structure: coarse-grained porphyritic to equigranular BG; 2) fine-grained pronouncedly porphyritic BG; and 3) aplites and pegmatites BG. In terms of petrochemical composition, BG are enriched in silica (71.3–75.1 wt% SiO<sub>2</sub>) and alkalis (7.7–8.9 wt% K<sub>2</sub>O + Na<sub>2</sub>O; K > Na). Elevated concentrations of Li, F, Rb, Cs, Sn, W, Nb, Ta, Pb, Y, HREE, and Th are characteristic. The content of Ba, Sr, and Zr in BG is lower than the crust abundance. The ratio (<sup>87</sup>Sr/<sup>86</sup>Sr)<sub>0</sub> = 0.7164 ± 0.0017 corresponds to crustal S-granites [4,5].

Quartz monzonites and monzogranites (MG) of the subalkaline series are composed of numerous small intrusions and medium-size massifs in the region (Inroginay, Lootaypin, and Palyan massifs). The MG dykes and stocks of the Ichuveem complex are localized in disjunctive structures, transverse to folding, and are closely associated with BG intrusions. Quartz monzonites and monzogranites are characterized by an increased alkalinity (7.9–9.1 wt%, and 8.0–9.3 wt% K<sub>2</sub>O + Na<sub>2</sub>O, respectively; K > Na) and by a relatively low silica content (66.2–69.7 wt%, and 68.5–70.4 wt% SiO<sub>2</sub>, respectively). Concentration of trace elements (Ti, P, W, Li, Sn, Cs, F, Zr, Y, and Yb) in MG is increased. Isotope-geochemical data indicate their crust-mantle origin [4,5].

Zinnwaldite granites (ZG) of the sub-alkaline series are microcline-albite granites with topaz, fluorite, and dark lithium mica. ZG belong to the rare-metal granite of the lithium–fluoric geochemical type. The area of ZG intrusions is located in the center of the Chaun district, where they transect the BG of the Severnyi and Pyrkanayan plutons and compose sills with a thickness of 1–2 m to several tens of meters. Sills of ZG are accompanied by pegmatoid veins with a thickness of 0.5–1 m. In the valley of the river Glubokaya, there is the small (3 km × 4 km) Kuluveem stock of medium-grained ZG. In the Severnyi Pluton, thin dikes of topaz–zinnwaldite ongonites have developed. ZG are distinguished by a high alumina content and alkalinity, reaching a maximum in ongonites [5]. A characteristic feature of ZG is the predominance of sodium over potassium, as well as the accumulation of Li, Rb, Cs, F, W, Ta, Nb, and other granitophilic elements. In addition to fluorine, boron plays a significant role in the composition of mineralizers. Deficiency of Sr, Ba, P, Zr, Ti, and Th, and a deep Eu anomaly, are observed. Intensive accumulation (more than five times clark) of Bi and Cs is a regional feature of the ZG of Chukotka. The tungsten concentration is ten times higher than the clark [4,5].

### 3. Materials and Methods

The paper presents the results of a study on the reference collection of granitoids collected during geological mapping of the central part of the Chaun district on a scale of 1:50,000, a total of more than 700 samples. Zircon has been studied in 220 specimens made from mineral concentrates and whole-rock specimens.

Information on the texture and composition of zircon was obtained by optical microscopy the Leica DM 2500M (Leica Microsystems, Wetzlar, Germany); the Olympus GX71 (OLYMPUS Co, Tokyo, Japan) cathodoluminescence and scanning electron microscopy the JSM-6460LV, and JSM-7001F (JEOL Ltd, Tokyo, Japan), and electron probe microanalysis the JXA-8230 (JEOL Ltd, Tokyo, Japan). We used the equipment of Saint-Petersburg Mining University. More than 600 electron probe and 100 ion probe analyzes were used to determine the concentrations of the constitutional components and trace elements in zircon. The texture of zircon was studied with more than 420 optical, 230 electronic, and 80 cathodoluminescent images. The methodology of this mineralogical research is described in [7].

Structural and chemical observations included optical selection of zircon grains, electron scanning, cathodoluminescence, as well as electron and ion sounding. The most important element of observations is the control of the mineral inclusions' presence. To compare the optical and electronic images, sample maps were used. Scanning was performed in SEM, TOPO, and COMPO modes with a sequential magnification from 100 to 300 to 5000 to 20,000. High-resolution scanning electron microscopy with thermal field emission and X-ray analyzers (JSM-7001F) made it possible to study grain inhomogeneities up to 6 nm in size with an image resolution of  $2560 \times 1920$ . For electronic sensing of zircon and related minerals, an INCA semiconductor detector (Oxford Instruments, England) was used: voltage: 15–25 kV; current 1.5 nA; analysis area: 3  $\mu\text{m}$ . The conditions for the wave dispersive spectrometry were an accelerating voltage of 20 kV, probe current of 100 nA, and the ZAF method of matrix effects correction.

Trace elements in zircon were determined by secondary ion mass spectrometry using a Cameca IMS-4f ion microprobe at the Yaroslavl' branch of the Institute of Physics and Technology of the Russian Academy of Sciences. The primary ion beam spot was 15–20  $\mu\text{m}$  in size; the relative error of trace element measurement was 10–15%; and the detection threshold of the elements was an average of 10 ppb. To construct the REE distribution spectra, the composition of zircon was normalized to that of chondrite CI [8].

#### 4. Results

The most important features of zircon as a mineral indicator are its morphology and composition [1–3]. Studies have shown that zircon of granitoid complexes of Northern Chukotka significantly differs in morphologic and geochemical features [4,5].

##### 4.1. BG Zircon

Zircon from BG is relatively large (150–500  $\mu\text{m}$  in length), euhedral, prismatic (elongation coefficient  $K_e = 2\text{--}4$ ), and with faces {110} and {111}. Two types of grains of zircon are distinguished. Zircon of the first, scarcer type is light yellow-brown, translucent, and with even smooth edges, and contains rare inclusions of monazite, xenotime, and thorite. The oscillatory zoning is characteristic: the thinnest zones 2–3  $\mu\text{m}$  thick are grouped into thicker (20–50  $\mu\text{m}$ ) zones that differ in luminous intensity. Zones are differed by lattice imperfection and composition of trace elements. Zircon of the second, predominant type is brown, opaque, and with an uneven relief of matte faces, and has mineral inclusions of thorite. Crystals are strongly recrystallized, homogeneous, or coarse-zoned; blocks with a primary oscillatory zonality are preserved in the core. The grains of BG zircon are surrounded by a metamict rim (light on BSE images; thickness 5–50  $\mu\text{m}$ ), enriched in isomorphic trace-elements and micro-inclusions of U, Th, Y, and HREE minerals (Figure 2a).

BG zircon of both types is characterized by a homogeneous distribution and low trace elements contents: 0.14–0.98 wt% Hf, 0.06–0.28 wt% Y, 0.03–0.29 wt% HREE, 0.02–0.12 wt% U, and 0.01–0.07 wt% Th (Table 1). The greatest accumulation of trace elements is observed in the rims of the crystals, where relatively large (5–15  $\mu\text{m}$ ) inclusions of xenotime, monazite, and uraninite are also observed. Small grains (1–3  $\mu\text{m}$ ) of the same minerals are found in rare dissolution voids and heterometric zircon cracks, which indicates their secondary nature. Uraninite and thorite are noted in the crystal nuclei inside the growth channels. The predominant trace elements are hafnium, yttrium, and heavy REE (mainly Yb, Er, and Dy) (Figure 3). The Th/U ratio is the highest: 0.27–1.79. The REE spectra in BG zircon reflect the predominant accumulation of heavy elements ( $\text{Lu}_N/\text{La}_N = 3894$ ,  $\text{Lu}_N/\text{Gd}_N = 22.4$ , and  $\text{Sm}_N/\text{La}_N = 51.5$ ). The anomalies of Eu ( $\text{Eu}/\text{Eu}^* = 0.01\text{--}0.05$ ) and Ce ( $\text{Ce}/\text{Ce}^* = 2.73\text{--}42.5$ ) are clearly pronounced (Table 2; Figure 4). In the rims enriched in rare metals, light REE are concentrated (mainly Ce, Sm, and Nd):  $\text{Sm}_N/\text{La}_N$  decreases to 1.7–2.7 [5,9].

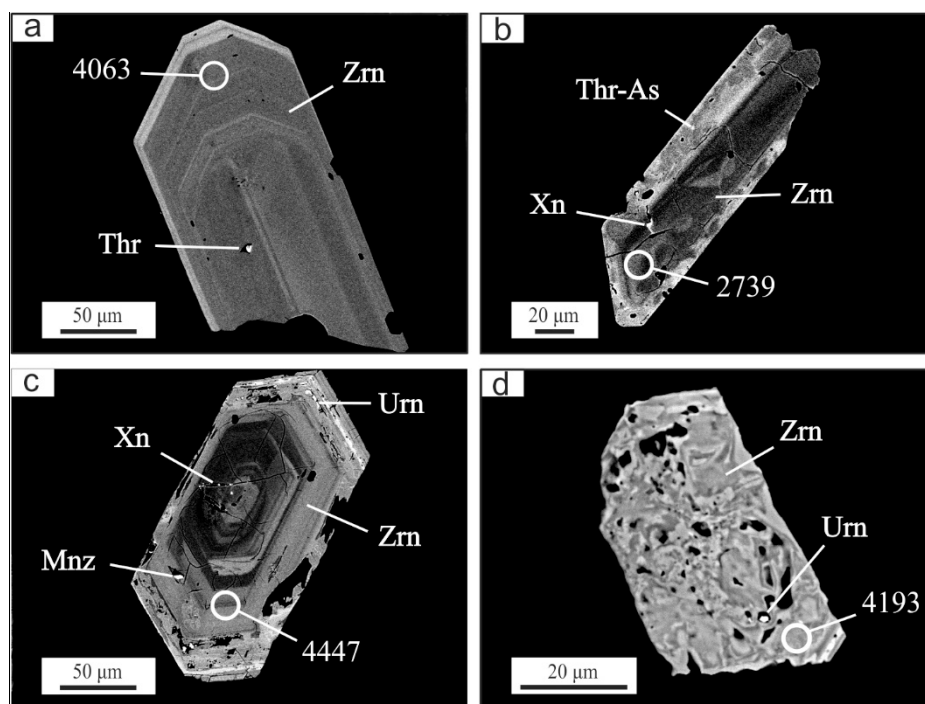


**Figure 2.** BSE images of typical zircon grains from granitoids of the Northern Chukotka. Numerals correspond to analyses in Table 1: (a) Euhedral, oscillatory zoned zircon of the second type in BG (coarse-grained equigranular granite, sample 4063, Table 1); (b) subhedral zircon of the second type with a bright rim enriched in U-Hf in MG (porphyric quartz monzonite, sample 2739, Table 1); (c) euhedral zoned zircon of the first type with a parental core, two bright rims strongly enriched in U and Hf in ZG (medium-grained zinnwaldite granite, sample 4447, Table 1); (d) subhedral patchy-zoned porous zircon of the second type rich in U, Hf, Y, and REE in ZG (microgranular albite-rich zinnwaldite granite, sample 4193, Table 1).

**Table 1.** Chemical composition of typical zircon from granitoids of the Chaun district, Chukotka.

Component	Biotite Granites			Monzonites, Monzogranites			Zinnwaldite Granites		
	4063	4105	BG	2739	9253	MG	4193	4447	ZG
EPMA, weight %									
SiO <sub>2</sub>	28.65	32.58	32.04	33.27	32.88	34.04	33.40	31.53	32.27
ZrO <sub>2</sub>	69.83	66.07	66.88	64.18	64.09	63.18	57.70	63.47	61.81
HfO <sub>2</sub>	0.17	0.85	0.60	1.20	1.67	1.61	5.99	2.46	3.78
ThO <sub>2</sub>	0.01	0.02	0.04	0.07	0.04	0.13	0.07	0.17	0.17
UO <sub>2</sub>	0.03	0.06	0.06	0.28	0.06	0.24	1.42	0.94	1.00
<b>Total</b>	<b>98.68</b>	<b>99.59</b>	<b>99.61</b>	<b>99.00</b>	<b>98.75</b>	<b>99.20</b>	<b>98.58</b>	<b>98.58</b>	<b>99.03</b>
SIMS, ppm									
Y	2452	1880	1818	2506	3884	2833	3140	3829	3904
ΣHREE	1147	913	758	1466	1663	2684	6481	5254	7151
ΣLREE	4.72	10.7	12.3	21.8	83.2	112	31.2	68.2	147
Al	b.d.l.	b.d.l.	b.d.l.	b.d.l.	377	251	566	b.d.l.	188
Ca	3.63	1.62	19.5	7.61	719	127	46.3	137	143
Ti	18.0	5.88	11.9	2.91	7.46	13.6	13.2	56.1	37.0
Nb	12.3	32.0	38.7	39.5	22.5	62.9	360	811	694
T(Ti), °C	798	698	758	645	718	771	768	922	873



Table 1. Cont.

Component	Biotite Granites			Monzonites, Monzogranites			Zinnwaldite Granites		
	4063	4105	BG	2739	9253	MG	4193	4447	ZG
<b>Structural Formulae, apfu</b>									
Si	0.911	1.000	0.997	1.022	1.014	1.035	1.042	0.989	1.006
Zr	1.083	0.989	1.004	0.961	0.963	0.937	0.884	0.970	0.939
Hf	0.002	0.008	0.005	0.011	0.015	0.014	0.053	0.022	0.034
Th	0.000	0.000	0.000	0.001	0.000	0.001	0.001	0.001	0.001
U	0.000	0.000	0.000	0.002	0.000	0.002	0.010	0.007	0.007
Y	0.004	0.003	0.003	0.004	0.006	0.005	0.005	0.006	0.007
ΣHREE	0.001	0.001	0.001	0.002	0.002	0.002	0.007	0.006	0.004
ΣLREE	0.000	0.000	0.000	0.000	0.000	0.000	0.000	0.000	0.000
Al					0.001	0.001		0.002	0.001
Ca	0.000	0.000	0.000	0.000	0.002	0.000	0.000	0.001	0.001
Ti	0.000	0.000	0.000	0.000	0.000	0.000	0.000	0.000	0.000
Nb	0.000	0.000	0.000	0.000	0.000	0.000	0.001	0.001	0.001

The composition of representative zircon samples of the Chaun (4063, 4105), Ichuveem (2739, 9253), and Pyrkakai (4193, 4447) granitoid complexes of Chukotka is presented. BG, MG, and ZG—the average composition of the zircon complexes (28, 32, and 71 samples, respectively); b.d.l.: below detection limits (Al: 0.1 ppm). ΣHREE = Gd + Di + Er + Yb + Lu. ΣLREE = La + Ce + Pr + Nd. T(Ti). °C—the zircon crystallization temperature [10]. The structural formulae were calculated on the basis of four atoms of oxygen.

#### 4.2. MG Zircon

Zircons from MG are of medium size (80–250 μm) and of two morphotypes. The crystals of the first, scarcer type are pale brown, euhedral, and columnar ( $K_e = 4-9$ ) or short-prismatic ( $K_e = 1-3$ ), with various dipyramids: {100} and, {111}, less often {110} and {112}. The edges of the prism {100} are smooth; the prisms {110} are stepped. The crystals of the second, predominant type are dark brown, subhedral, with rounded peaks and edges: {110} and {112}. Their inner part is recrystallized and porous, and the outer rim is concentrically zoned (Figure 2b).

MG zircon is characterized by elevated concentrations of trace elements: 1.12–2.11 wt% Hf, 0.04–0.43 wt% Y, 0.08–0.45 wt% HREE, 0.04–0.57 wt% U, and 0.03–0.35 wt% Th. The elements that are rare in zircon, such as Al, Ca, and Nb, appear sporadically in quantities of up to 0.25, 0.1, and 0.04 wt%, respectively (Table 1). All isomorphic elements are distributed unevenly. The highest levels of trace elements are observed in the outer rim. Its specific feature is a relatively high concentration of hafnium and actinoids (Figure 3). The Th/U ratio is moderate: 0.15–1.50. An increase in the content of thorium and yttrium is accompanied by micron inclusions of arsenic-containing thorite and xenotime in the pores and cracks. As–thorite micro-veinlets with a thickness of 0.2–0.5 μm were found. The crystals of the second type are distinguished by a high content of Hf and U, and by a dark brown color due to poikilitic inclusions in the core of the uraninite, thorite, apatite, and REE-U minerals.

The REE distribution in MG zircon is characterized by a positive correlation of the content and atomic weights of the elements:  $Lu_N/La_N = 524$ ,  $Lu_N/Gd_N = 21.2$ , and  $Sm_N/La_N = 7.91$ . Average anomalies:  $Eu/Eu^* = 0.08$  and  $Ce/Ce^* = 2.96$  (Table 2; Figure 4). At the periphery of the crystals, the content of LREE increases. It concerns primarily Ce, Pr, and Nd ( $Sm_N/La_N = 3.0-29.8$ ) [5].

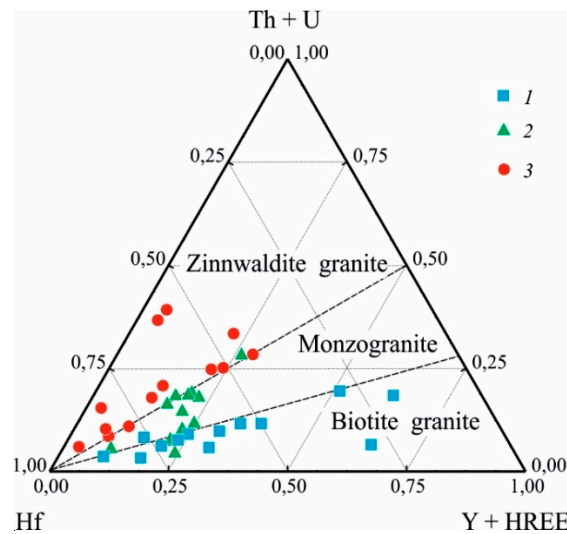


**Figure 3.** The ratio of the main trace elements in the zircon granitoids of the Chaun region, Northern Chukotka: 1—biotite granites, 2—quartz monzonites and monzogranites, 3—zinnwaldite granites.

**Table 2.** Rare earth composition of typical zircon from granitoids of the Chaun district, Chukotka.

REE	Biotite Granites			Monzonites, Monzogranites			Zinnwaldite Granites		
	4063	4105	BG	2739	9253	MG	4193	4447	ZG
La	0.23	0.08	0.43	0.68	9.13	9.24	2.67	7.29	10.8
Ce	2.12	9.09	8.92	16.5	40.7	60.8	14.3	35.4	82.7
Pr	0.14	0.12	0.28	0.44	4.86	5.90	1.92	4.24	8.26
Nd	2.23	1.42	2.61	4.26	28.5	36.4	12.4	21.2	46.0
Sm	4.53	4.05	4.30	6.18	20.6	30.1	20.3	26.1	53.9
Eu	0.20	0.11	0.09	0.40	0.80	1.47	0.25	0.35	0.54
Gd	27.6	24.3	21.5	33.3	67.4	93.4	61.5	65.3	145
Dy	132	115	95.6	150	220	349	382	418	740
Er	317	255	206	378	477	715	1120	1067	1622
Yb	573	451	377	779	783	1327	4204	3197	4049
Lu	96.9	66.8	58.7	126	115	200	714	506	595
<b>Ratios of Chondrite-Normalized Zircon REE Patterns</b>									
Eu/Eu*	0.06	0.03	0.03	0.08	0.07	0.08	0.02	0.03	0.02
Ce/Ce*	2.91	22.0	16.2	7.23	1.48	2.96	1.53	1.54	2.03
Lu <sub>N</sub> /La <sub>N</sub>	4132	7792	3894	1775	121.9	524	2577	668	803
Lu <sub>N</sub> /Gd <sub>N</sub>	28.4	22.2	22.4	30.6	13.9	21.2	94.0	62.7	42.7
Sm <sub>N</sub> /La <sub>N</sub>	32.1	78.6	51.5	14.5	3.61	7.91	12.2	5.74	8.79

The composition of representative zircon samples (see Table 1). Chondrite values are from [8]. Eu and Ce anomalies were calculated in this manner:  $Eu/Eu^* = Eu_N / (\sqrt{Sm_N \times Gd_N})$ .

### 4.3. ZG Zircon

Zircon from ZG is notable for its small size (20–100 μm), short-prismatic ( $K_c = 1.5–3$ ) crystals with blunt dipyrmidal vertices—{110}, {111}, {112}, and {113}—and a bumpy relief of the faces. The internal texture is complex: There is a core and relatively wide rims enriched with heavy elements and visible on the BSE images. Two types of zircon are distinguished: the first, scarcer type with oscillatory zones, and the second, predominant type with a recrystallized core. Zircon of the second type and the outer rim in the crystals of the first type have a defective crystal structure, manifested in a weakened CL glow. In these parts of the crystals, the growth zonality is impaired, and secondary sinuous zones and homogeneous recrystallized blocks with indeterminate boundaries predominate. Due to the sharp structural mismatch between the inner part, the rims, and the recrystallized sections, radial fractures of heterometry and numerous irregular pores of various sizes (0.05–5.0 μm) and lenticular cavities (up to

10–50  $\mu\text{m}$ ) are developed at their boundaries. The volume of the voids reaches 1–5% of the grain volume. In the pores there are foreign minerals 0.5–5  $\mu\text{m}$  in size: topaz, fluorite, fluocerite-(Ce), monazite-(Ce), uraninite, thorite, As-thorite, xenotime-(Y), yttrialite-(Y), uranosphaerite, and cerianite-(Ce). ZG zircon contains a large number of gas–liquid inclusions and mineral inclusions of U, Th, Y, and REE restricted to the outer rim (Figure 2c). Zircon of zinnwaldite microgranites (ongonites) is represented by the same morphotypes, but grains of the second type predominate (85%): small (less than 10  $\mu\text{m}$ ) porous crystals with a rough relief of faces, dark in cathodoluminescence. The appearance of zircon is shortened, with uneven edges. Rough-zonal and domain internal texture, metamictization, and numerous mineral micro-inclusions are common (Figure 2d).

ZG zircon stands out for its high content of heavy trace elements, reflected in the increased brightness of the BSE images (Figure 2): 2.37–9.82 wt% Hf, 0.18–1.71 wt% U, 0.04–1.15 wt% HREE, 0.07–0.91 wt% Y, and 0.01–0.50 wt% Th (Table 1). A characteristic feature of zircon ZG is its coarse triple zonality, complicated by oscillatory fluctuations of the contents of Hf, U, Th, and REE (Yb, Er, and Dy, as well as Ce and Nd). The core “uranium zone” and “hafnium border” of 5–20  $\mu\text{m}$  are distinguished. The core is, apparently, a protocrystal, recrystallized to a variable degree and relatively poor in trace elements. The middle zone (10–30  $\mu\text{m}$ ) is most abundant in U, Th, REE, and other elements that are rare in zircon, such as Ca, Al, LREE, and micro-inclusions of thorite, uraninite, xenotime-(Y), and monazite-(Ce). The outer rim with a thickness of 5–20  $\mu\text{m}$  is saturated with hafnium: the Zr/Hf ratio reaches 5.9. On the periphery, as in the core, oscillatory zoning is often observed.

Typical trace-elements of ZG zircon are hafnium, uranium, and thorium (Figure 3). In the hafnium zone, Nb (up to 0.26%) and Ti (up to 0.03%) accumulate; in the uranium zone—LREE (up to 0.02%). The outer zones contain elements uncharacteristic of zircon: Ca up to 0.05%, and Al up to 0.17% (Table 1, sample 4447). The Th/U ratio is the lowest: 0.01–0.46. The highest concentrations of rare elements are observed in recrystallized, cavernous crystals of zircon from ZG of the second type (Figure 2d). The distinction between the core, uranium, and hafnium zones almost disappears. The spotted-zonal texture of the grains is characteristic; the content of the trace elements fluctuates sharply along the growth zones, but generally grows to the periphery. The REE spectra in ZG zircon have a positive slope:  $\text{Lu}_N/\text{La}_N = 803$ ,  $\text{Lu}_N/\text{Gd}_N = 42.7$ , and  $\text{Sm}_N/\text{La}_N = 8.79$ . The average values of the anomalies are  $\text{Eu}/\text{Eu}^* = 0.02$  and  $\text{Ce}/\text{Ce}^* = 2.03$  (Table 2, Figure 4). In the uranium zone of the crystals, the content of Ce, Pr, and Nd increases: the  $\text{Sm}_N/\text{La}_N$  ratio decreases to 3.15–16.6 [5,9].



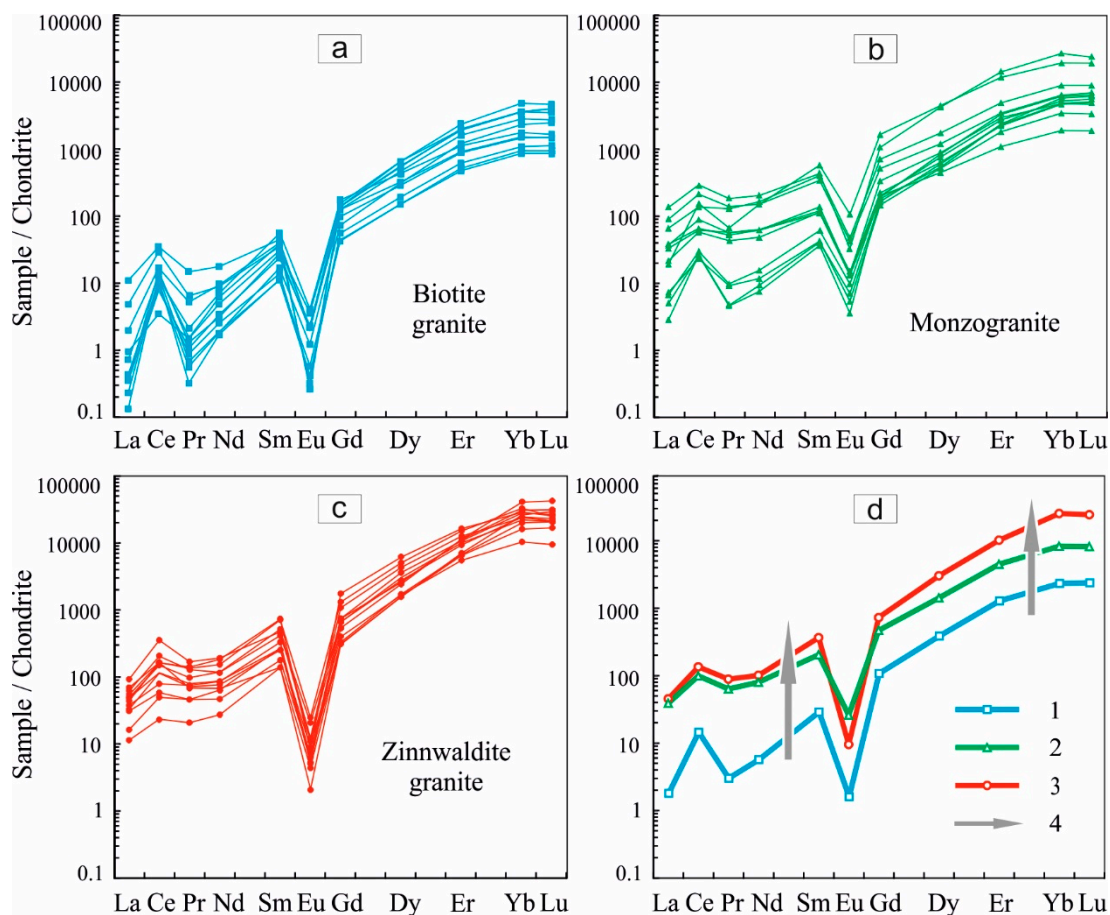


**Figure 4.** Chondrite-normalized rare earth element patterns for zircon from granitoids of the Chaun district, Northern Chukotka: (a–c) BG, MG, and ZG, respectively; (d) average normalized concentrations of REE: 1—BG, 2—MG, 3—ZG, 4—the trend in REE evolution. Chondrite values are from [8].

## 5. Discussion

### 5.1. Morphology of Zircon

Zircon in granitoids of different stages of magmatism in Northern Chukotka clearly differs in shape and texture and forms a generation series, which includes populations of three consecutive intrusive complexes—biotite granites, quartz monzonites, and zinnwaldite granites. BG zircon has a relatively large size, and the typical zircon appearance, texture, and composition of a magmatic-type zircon. The absence of detritic seeds and the features of morphology suggest its high-temperature crystallization in primary magma reservoirs depleted in rare elements [5]. Signs of recrystallization and the presence of an external zone in zircon of the second type indicate its post-magmatic transformation under the influence of late MG, ZG, and their fluids (Figure 2).

MG zircon has a mean size and columnar habit, indicating magmatic crystallization [11]. It is formed by the regeneration of a parental zircon or crystallization of a melt with increased alkalinity and water saturation. The poorly faceted cyrtolite of the second type and the rim of crystals of the first type are formed under relatively low temperature conditions with significant participation of fluids [5].

ZG zircon is the smallest, has a barrel-shaped habit, and a very complex morphology and texture, indicating a deep transformation and regeneration of zircon protocrytals or direct low-temperature crystallization in a fluid-saturated melt [11]. Based on its composition, zircon of the first type is a product of regenerated parental zircon. The second type is formed during the recrystallization of grains of the first type or by primary crystallization in the melt [5]. The formation of wide rare-metal rims of zircon occurs with an increase in the alumina content of the melt. Pores and the mineral inclusions

located in them are formed due to the dissolution of the mineral by fluids of increased alkalinity, as well as the capture of fluid inclusions by zircon [1,5,11,12].

Thus, in the rock series BG → MG → ZG, there is a decrease in the size and elongation of accessory zircon (average size 330 → 170 → 60 μm), complication of the relief of the faces, and a change in morphology: domatic zircon → columnar habit → barrel-shaped habit. At the same time, there is a complication of the structure of zircon crystals: an increase in the degree of recrystallization and heterometric deformation, the proportion of porosity, and power of the outer rare-metal rim. In zircons of late granitoids, protolithic relics are recorded: Crystals of the first type are formed during the regeneration and change of grains extracted from the substrate of the magma chamber. In MG and ZG, there is a syngenetic zircon of the second type with complex texture of pores and mineral inclusions. From early to late granitoids, the size naturally decreases, whereas the number and species diversity of the mineral inclusions in zircon increase.

Indicator morphological signs of the zircon of granitoids at the stages of granitoid magmatism in Northern Chukotka are the size, elongation, habit, and texture of the crystals. The evolution of the mineral is explained by an increase in the fluid saturation and alkalinity of the granite magma over time. It can be assumed that the initial crystallization depth of the zircon decreases from biotite granites and quartz monzonites to zinnwaldite granites [11,13].

### 5.2. Composition of Zircon

Zircon in the granitoids of the Northern Chukotka varies in composition due to differences in the magmatic differentiation and post-magmatic transformation of the rocks. BG zircon is characterized by a low content of trace elements, mainly Hf, Y, and HREE (Tables 1 and 2; Figure 3). The mineral is relatively poor in uranium (Figure 5) and has a high (up to 1.79) Th/U ratio. It was formed by crystallization in a granite melt depleted in rare elements [1,9,12]. The zircon crystallization temperature was determined by the Ti-in-Zrn thermometer [10]. The temperature values of the BG zircon range between 679 and 831 °C (Table 1). It has a magmatic type of REE spectrum with Ce and Eu anomalies, and the predominant accumulation of HREE (Figure 4).

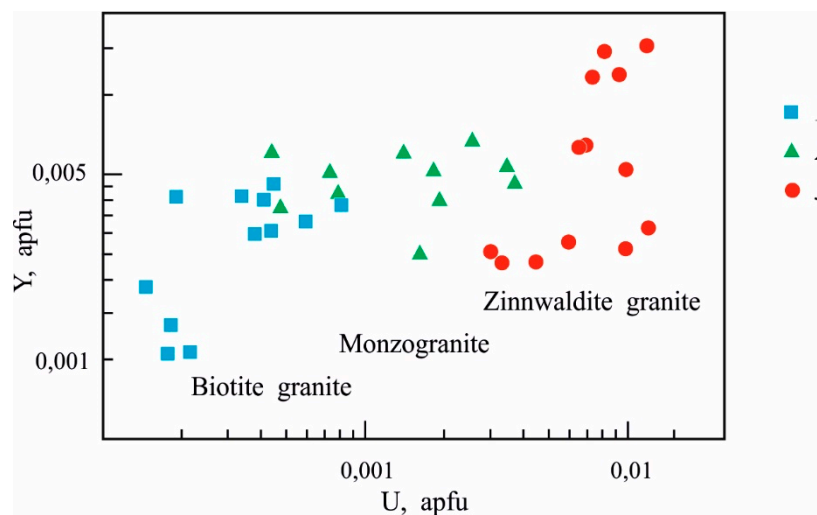


**Figure 5.** The ratio of U and Y cations in zircon of granitoids in the Chaun region, Northern Chukotka. For notation keys, see Figure 3.

MG zircon, in comparison with BG zircon, accumulates more Hf, Y, HREE, U, and Th (Tables 1 and 2; Figures 3–5). An outer rim enriched with rare elements appears. Elements that are rare in zircon are as follows: in the core—Al, Ca, and Nb; and in the rim—LREE and As. Typical trace-elements of MG zircon are LREE and Th. An identifying feature is the presence of mineral inclusions: As-thorite, xenotime, uraninite, thorite, etc. The enrichment of rare metals indicates a

specialization of monzogranite melts, which grows in the late stages of zircon crystallization. The MG zircon crystallization temperatures range between 645 and 934 °C (Table 1).

ZG zircon, representing a cyrtolite, contains the maximum amount of trace elements, about 2.68–14.38 wt% (Table 1). The proportion of isomorphous components increases stepwise from the core to the margin, and the pattern noted in ZG zircon of the Far East is confirmed: We observed a core captured from the parental granite melt and double rims—inner uranium and outer hafnium [5]. The uranium rim is enriched in U, Th, and HREE, and microminerals of these elements, as well as Ca and Al; hafnium border: Hf, Nb, and Ti (Table 1; Figures 3 and 5). The composition of REE in ZG zircon is dominated by Yb, Er, and Dy; Ce and Eu anomalies are more intense compared to zircon from previous granitoids (Table 2; Figure 4). The Th/U ratio is the lowest: up to 0.06. Typical trace elements in ZG zircon are Hf, U, HREE, Nb, Ti, Al, and Ca (Tables 1 and 2). Mineral inclusions are more diverse: monazite, xenotime, uraninite, thorite, fluorite, topaz, etc.

A distinct rare-metal specialization of the ZG zircon formation medium is observed. The distribution of trace elements in cyrtolite is explained by the geochemical evolution of magma: U, Y, HREE, Th → Hf, Nb, and LREE (Table 1). A change in the composition of magma occurs upon its differentiation, an increase in alumina and alkalinity, which determines the accumulation of rare elements in the residual melt [2]. Morphology, the thin growth zonality of the hafnium rim, excludes the hydrothermal origin of ZG cyrtolite. The inhomogeneous distribution and the presence of uncommon elements, the accumulation of LREE, and the deepening of the Eu anomaly indicate late magmatic crystallization in a fluid-saturated melt [1,12–14]. The value of the crystallization temperature calculated by the Ti-in-zircon thermometer [10] for ZG zircon varies from 634 to 1060 °C. The composition of late magmatic ZG zircon resembles the composition of hydrothermal zircon. The capture of uncommon elements contributes to the imperfection of the crystal structure of cyrtolite. In the composition, it corresponds to the zircon of rare-metal subalkaline granites in the Erzgebirge of Europe, in Jiangxi Province of China, and the Eastern Desert in Africa [2,15–18].

Thus, in the rock series BG → MG → ZG, there is a sharp explosive increase in the diversity and concentration of isomorphous trace elements and micro-inclusions in zircon, which reflects a change in the composition of the granitoid magmas. The distribution of trace elements in the zircon crystals is also complicated. The homogeneous distribution of a small amount of trace elements in BG zircon is replaced by the zonal distribution “core–rare metal rim” in MG zircon and “core–U-rim–Hf-rim” in ZG zircon. A specific expression of the geochemical evolution of zircon in this series is the concentration trends of U, Y, HREE, Th, Hf, Nb, LREE, Ti, Ca, and Al (Figures 3 and 4). The accumulation of light REE is probably associated with an increase in the role of fluids in the process of heterogenization of fluorine-containing granite magma [12]. The deepening of the europium anomaly reflects an increase in the oxidation of mineral-forming melts [13].

In the discriminatory diagram “Y vs. U” [14], there is a clear separation of the figurative points of BG, MG, and ZG zircons within the granitoid field (Figure 5). The evolutionary increase in the content of U and Hf in zircon of the successively formed granitoids BG → MG → ZG is reflected in the change of the Zr/Hf ratios—>100, 50–100, and 15–50—respectively; and Th/U— >0.3, 0.15–1.5, and 0.01–0.5—respectively. This allows us to propose Zr/Hf vs. Th/U for the discrimination of granitoids of various stages of magmatism in Northern Chukotka (Figure 6).

Thus, the evolution of accessory zircon is reflected in the history of the Late Cretaceous granitoid magmatism of Northern Chukotka. A typical zircon of the weakly differentiated, calc-alkaline granites in BG is replaced by zircon enriched with Th and LREE in MG subalkaline granites. The process ends with the formation of zircon of ore-bearing subalkaline rare-metal ZG granites, bearing significant concentrations of Hf, U, Y, HREE, Nb, and Ti (Tables 1 and 2; Figures 3–5).

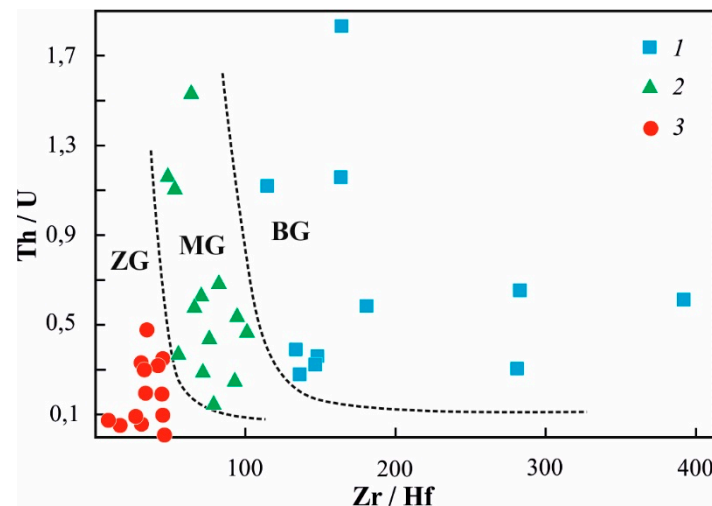


**Figure 6.** The difference in the composition of zircon on the diagram of Zr/Hf vs. Th/U in granitoids of various magmatism stages in the Chaun region, Northern Chukotka. For notation keys, see Figure 3.

## 6. Conclusions

The paper shows that the morphology, texture, and composition of accessory zircon, serving as reliable signs of granitoids in the three magmatism stages in the Chaun region of Northern Chukotka. In the rock series BG → MG → ZG, the morphological evolution of zircon occurs: a decrease in size and elongation, and the complication of crystal habits. In the later generations of zircon, due to the processes of recrystallization, metasomatism, deformation, and crystallization of the mineral inclusions, we observe the appearance of rare-metal rims, defects in the crystal structure, mineral inclusions and pores, and complication of the indexes and faces relief.

In a series of Chukotka granitoids, the geochemical evolution of zircon is observed. The stepwise increase in the content of rare elements (Hf, U, Y, Th, REE, Nb, and Ti) is established. Rare elements (REE, Y, Hf, Nb, U, and Th) at the post-magmatic stage of the region's history acquire industrial significance; therefore, zircon serves as a sign of productive ore-magmatic systems [5]. The extraction of trace elements during the decomposition of zircon and mineral inclusions at the post-magmatic stage leads to the enrichment of hydrothermal solutions with rare elements. Thus, zircon of rare-metal granites plays the geochemical role of an intermediate concentrator of ore elements and is considered to be an indicator of ore-bearing granites.

**Author Contributions:** Conceptualization, V.I.A.; methodology, V.I.A.; software, V.I.A.; validation, V.I.A.; formal analysis, V.I.A.; investigation, V.I.A.; resources, V.I.A.; data curation, V.I.A. and I.V.A.; writing—original draft preparation, V.I.A.; writing—review and editing, I.V.A.; visualization, V.I.A. and I.V.A. All authors have read and agreed to the published version of the manuscript.

**Funding:** This research received no external funding.

**Acknowledgments:** The authors extend appreciation to S.G. Simakin and E.V. Popov (IPT RAS, Yaroslavl), as well as I.M. Gembitskaya (SPMU, Saint-Petersburg) for analytical studies.

**Conflicts of Interest:** The authors declare no conflict of interest.

## References

- Hoskin, P.W.O.; Schaltegger, U. The composition of zircon and igneous and metamorphic petrogenesis. *Rev. Miner. Geochem.* **2003**, *53*, 27–62. [[CrossRef](#)]
- Kempe, U.; Gruner, T.; Renno, A.D.; Wolf, D.; Reno, M. Discussion on Wang (2000). Chemistry of Hf-rich zircons from the Laoshan I- and A-type granites, Eastern China. *Min. Mag.* **2004**, *68*, 669–675. [[CrossRef](#)]
- Harley, S.L.; Kelly, N.M. Zircon. Tiny but Timely. *Elements* **2007**, *3*, 13–18. [[CrossRef](#)]
- Goryachev, N.A. Chukotka plutonic belt (late Jura — Cretaceous). *Geodyn. Magmat Metallog. Russ. East* **2006**, *1*, 230–242. (In Russian)

5. Alekseev, V.I. *Lithium-Fluoric Granites of the Far East*; Saint-Petersburg Mining University: St. Petersburg, Russia, 2014; pp. 1–244. (In Russian)
6. Nokleberg, W.J.; Parfenov, L.M.; Monger, J.W.H.; Norton, I.O.; Khanchuk, A.I.; Stone, D.B.; Scotese, C.R.; Scholl, D.W.; Fujita, K. Phanerozoic tectonic evolution of the Circum-North Pacific. *USGS Prof. Paper* **2000**, *1626*, 1–122.
7. Brodskaya, R.L.; Marin, Y.B. Ontogenetic analysis of mineral grains and aggregates at micro- and nanolevel for the restoration of ore-forming conditions and assessment of mineral raw technological properties. *J. Min. Inst.* **2016**, *219*, 369–376. (In Russian)
8. McDonough, W.F.; Sun, S.-S. The composition of the Earth. *Chem. Geol.* **1995**, *120*, 223–253. [[CrossRef](#)]
9. Alekseev, V.I.; Marin, Y.B.; Skublov, S.G.; Gembitskaya, I.M. First data on chemical composition of zircon from lithium–fluorine granite of the Severnyi Pluton, Chukchi Peninsula. *Geol. Ore Depos.* **2012**, *54*, 570–574. [[CrossRef](#)]
10. Watson, E.B.; Wark, D.A.; Thomas, J.B. Crystallization thermometers for zircon and rutile. *Contrib. Miner. Petrol.* **2006**, *151*, 413–433. [[CrossRef](#)]
11. Pupin, J.P. Zircon and granite petrology. *Contrib. Miner. Petrol.* **1980**, *73*, 207–220. [[CrossRef](#)]
12. Pelleter, E.; Cheilletz, A.; Gasquet, D.; Mouttaqi, A.; Annich, M.; El Hakour, A.; Deloule, E.; Féraud, G. Hydrothermal zircons: A tool for ion microprobe U–Pb dating of gold mineralization (Tamlalt–Menhouhou gold deposit – Morocco). *Chem. Geol.* **2007**, *245*, 135–161. [[CrossRef](#)]
13. Pettke, T.; Audétat, A.; Schaltegger, U.; Heinrich, C.A. Magmatic-to-hydrothermal crystallization in the W–Sn mineralized Mole Granite (NSW, Australia). Part II: Evolving zircon and thorite trace element chemistry. *Chem. Geol.* **2005**, *220*, 191–213. [[CrossRef](#)]
14. Belousova, E.A.; Griffin, W.L.; O’Reilly, S.Y.; Fisher, N.I. Igneous zircon: Trace element composition as an indicator of source rock type. *Contrib. Miner. Petrol.* **2002**, *143*, 602–622. [[CrossRef](#)]
15. Huang, X.L.; Wang, R.C.; Chen, X.M.; Hu, H.; Liu, C.S. Vertical variations in the mineralogy of the Yichun topaz-lepidolite granite, Jiangxi Province, southern China. *Can. Mineral.* **2002**, *40*, 1047–1068. [[CrossRef](#)]
16. Johan, Z.; Johan, V. Accessory minerals of the Cínovec (Zinnwald) granite cupola, Czech Republic: Indicators of petrogenetic evolution. *Mineral. Petrol.* **2005**, *83*, 113–150. [[CrossRef](#)]
17. Breiter, K.; Föörster, H.-J.; Škoda, R. Extreme P-, Bi-, Nb-, Sc-, U- and F-rich zircon from fractionated perphosphorons granites: The peraluminous Podlesí granite system, Czech Republic. *Lithos* **2006**, *88*, 15–34. [[CrossRef](#)]
18. Abdalla, H.M.; Helba, H.; Matsueda, H. Chemistry of zircon in rare metal granitoids and associated rocks, Eastern Desert, Egypt. *Resour. Geol.* **2009**, *59*, 51–68. [[CrossRef](#)]

